Published in final edited form as:
*Alcohol Clin Exp Res*. 2014 July ; 38(7): 2008–2014. doi:10.1111/acer.12464.

# Dysmorphogenic effects of first trimester equivalent ethanol exposure in mice: a magnetic resonance microscopy-based study

**Scott E. Parnell**[1,2,*], **Hunter E. Holloway**[1], **Lorinda K. Baker**[1], **Martin A. Styner**[3,4,5], and **Kathleen K. Sulik**[1,2,5]

[1]University of North Carolina - Bowles Center for Alcohol Studies, Chapel Hill, North Carolina, United States

[2]University of North Carolina - Department of Cell Biology and Physiology, Chapel Hill, North Carolina, United States

[3]University of North Carolina - Department of Psychiatry, Chapel Hill, North Carolina, United States

[4]University of North Carolina - Department of Computer Science, Chapel Hill, North Carolina, United States

[5]University of North Carolina - Carolina Institute for Developmental Disabilities, Chapel Hill, North Carolina, United States

## Abstract

**Background—**The first trimester of human development and the equivalent developmental period in animal models is a time when teratogenic ethanol exposure induces the major structural birth defects that fall within Fetal Alcohol Spectrum Disorder (FASD). Previous FASD research employing an acute high dose maternal intraperitoneal ethanol treatment paradigm has identified sensitive periods for a number of these defects. Extending this work, this investigation utilized high resolution magnetic resonance imaging (MRM)-based analyses to examine the dysmorphology resulting from maternal dietary ethanol intake occurring during selected first trimester-equivalent time periods.

**Methods—**Female C57Bl/6J mice were acclimated to a liquid 4.8% ethanol (v/v)-containing diet, then bred while on standard chow. Dams were again provided the ethanol-containing liquid diet for a period that extended either from the beginning of gestational day (GD) 7 to the end of GD 11 or from the beginning of GD 12 to the end of GD 16. On GD 17, a subset of fetuses was selected for MRM-based analyses. Group comparisons were made for litter characteristics and gross dysmorphology, as well as whole and regional brain volumes.

**Results—**Ethanol-induced stage of exposure-dependent structural brain abnormalities were observed. The GD 7–11 ethanol-exposed group presented with a significant decrease in cerebellar volume and an increase in septal volume, while GD 12–16 ethanol treatment resulted in a

[*]To whom correspondence should be addressed:, Scott E. Parnell, Ph.D., University of North Carolina, Bowles Center for Alcohol Studies, CB #7178, Chapel Hill, NC 27599, United States, Tel: 919-966-3208, Fax: 919-966-5679, sparnell@med.unc.edu.

reduction in right hippocampal volume accompanied by enlarged pituitaries. Additionally, the GD 12–16 ethanol exposure caused a high incidence of edema/fetal hydrops.

**Conclusions—**These results illustrate the teratogenic impact of maternal dietary ethanol intake occurring at time periods approximately equivalent to weeks 3 through 6 (GD 7–11 in mice) and weeks 7 through 12 (GD 12–16 in mice) of human gestation, further documenting ethanol's stage of exposure-dependent neuroteratogenic endpoints and highlighting the vulnerability of selected brain regions during the first trimester. Additionally they suggest that clinical attention should be paid to fetal hydrops as a likely component of FASD.

**Keywords**

Fetal Alcohol Spectrum Disorder; Magnetic Resonance Imaging; Mouse; Brain; Ethanol

## INTRODUCTION

Studies of Fetal Alcohol Spectrum Disorder (FASD) animal models have illustrated that the type and severity of ethanol-induced birth defects are largely dependent upon the treatment pattern and dosage along with the developmental stage of the conceptus at the time of ethanol exposure. While virtually all stages of embryonic and fetal development are vulnerable to the teratogenic effects of ethanol (Maier et al., 1999, Mooney and Miller, 2009, Livy, 2003, Sawant et al., 2013, Schneider et al., 2011), it is during the human first trimester-equivalent that most of the major structural abnormalities of the face, brain, and other organ systems are induced (Sulik, 2005). Given that most prenatal ethanol exposure occurs during the human first trimester, it is especially important to fully understand the teratogenic end points resulting from maternal ethanol use during this period (Floyd et al., 1999, Cornelius et al., 1993, Coles et al., 1985).

In rodents, the human first trimester-equivalent encompasses much of the prenatal period, with sensitivity to ethanol-induced gross structural changes beginning as early as gestational day (GD) 7, when mouse embryonic stages are consistent with those in the human 3$^{rd}$ week post-fertilization (Sulik et al., 1981). As evidenced, in part, by the appearance of long bone ossification centers and closure of the secondary palate, transition from the embryonic to fetal period occurs at the beginning of the 9$^{th}$ week in humans and at approximately the 14$^{th}$ to 15$^{th}$ day in mice, (Schoenwolf et al., 2009, Otis and Brent, 1954, Strachan et al., 1997). While there are no commonly recognized features that distinguish the embryonic versus fetal periods of brain development, the overall morphology of the mouse and human brain is very similar at the time of transition between these developmental stages (Theiler, 1989, Kaufman, 1992, O'Rahilly and Fabiola, 1992). Although differences do occur between mice and humans in the developmental rate of various organ systems [including the brain which also has regional interspecies differences (Workman et al., 2013)], overall the 12 week time period of which the human first trimester is comprised appears roughly equivalent in the mouse to the period extending to and probably through the 16$^{th}$ day of gestation. Thus, based on developmental events, approximately half of the human second trimester-equivalent as well as all of the third trimester-equivalent occur after the 19–21 day gestation period in the mouse.

The ability to comprehensively examine the structural changes that prenatal ethanol exposure causes has been facilitated with the application of advanced imaging methodologies, especially magnetic resonance microscopy (MRM; high resolution magnetic resonance imaging) to the study of fetal mice. This is exemplified by studies examining GD 17 fetuses and focusing on the effects of binge-like, high-dose maternal ethanol treatment limited to each of GDs 7, 8, 8.5, 9, and 10. Exposure stage-dependent neuroanatomical and craniofacial abnormalities that are consistent with those in Fetal Alcohol Syndrome (FAS) and FASD (Lipinski et al., 2012, Godin et al., 2010, O'Leary-Moore et al., 2010, Parnell et al., 2009) have been described. Included among the defects are volumetric and shape changes in the septal region of the forebrain, the striatum, pituitary, hippocampus, and cerebellum, as well as cerebro-cortical heterotopias, hypothalamic hamartomas, ventricular enlargement, and corpus callosum deficiencies.

While the high binge exposure-based results reported to date have aided in pinpointing sensitive periods for a variety of ethanol-induced malformations, a first trimester equivalent-focused study of the teratogenic sequelae of an ethanol exposure regimen more typical of human consumption was considered warranted. To this end, a repeated maternal ethanol exposure paradigm employing volitional dietary intake and MRM-based fetal examination was employed. Furthermore, to test the hypothesis that with this exposure paradigm, early versus late human 1$^{st}$ trimester-equivalent exposures yield differing patterns of structural malformations, ethanol-containing diet was made available to dams for 5 day periods extending from GDs 7 through 11 or 12 through 16. These time periods correspond respectively to approximately the 3$^{rd}$ through the 6$^{th}$ and the 7$^{th}$ through 12$^{th}$ weeks of human prenatal development.

## MATERIALS AND METHODS

### Animal Husbandry & Maternal Ethanol Exposure

Male and female C57Bl/6J mice were obtained from The Jackson Laboratory (Bar Harbor, ME) at approximately 10 weeks of age. The mice were housed in a reverse light/dark cycle room (lights off at 9 am and on at 9 pm), and except when provided liquid diet as their sole source of calories, they were given standard laboratory chow and water ad libitum. The liquid diet (PMI microstabilized ethanol rodent liquid diet) is a modified Lieber-DeCarli formula obtained from Test Diet (Richmond, IN), with 5% sucrose added to increase palatability (Parnell et al., 2006). Prior to pregnancy, the female mice were acclimated for 2 days to the liquid diet containing 2.4% ethanol (v/v). For the following 6 days, the mice were provided the liquid diet containing 4.8% ethanol (v/v). Subsequent to this acclimation period, the mice were returned to their chow diet for 2–3 days and then bred by putting one female with one male mouse for a 1 hr period. The beginning of this breeding period was designated as gestational day (GD) 0 for those mice in which a copulation plug was found. As described previously in Parnell et al., (2006), ethanol acclimation prior to breeding is necessary to ensure that even on the first day of return to the ethanol-containing liquid diet, the pregnant mice will consume enough to reach a peak BEC of ~200 mg/dl.

The acclimated pregnant mice were randomly assigned to either the ethanol-exposed or control group. The dams in the ethanol-exposure groups were again provided the 4.8% (v/v)

ethanol-containing liquid diet for a five day period that extended either from the beginning of GD 7 to the end of GD 11 (GD 7–11 group) or from the beginning of GD 12 to the end of GD 16 (GD 12–16). The control groups were provided access to the liquid diet with an isocaloric amount of maltodextrin in place of ethanol. To control for potential dietary effects, the volume of liquid diet consumed by each ethanol-exposed mouse was recorded daily and the controls were matched to their respective ethanol group by restricting the volume of diet based on ml diet/g body weight.

## Fetal Specimen Collection & Magnetic Resonance Microscopy (MRM)

On GD 17, control and ethanol-exposed fetal mice were collected following euthanasia of the dam, numbers of live and dead fetuses and resorptions in each uterus were recorded, and extraembryonic membranes were removed. With the exception of 2 obviously edematous fetuses in the GD 12–16 ethanol-exposed group, which were chosen to further explore ethanol-induced edema, the fetuses to be examined employing MRM were chosen without regard to gross morphology. Other than three fetuses in the GD 12–16 control group, no more than two fetuses per litter were selected in order to avoid any potential litter effects. The chosen specimens were photographed and then drop-fixed in a 20:1 Bouin's fixative (Sigma Aldrich, St. Louis, MO):Prohance (Bracco Diagnostics, Princeton, NJ) solution for 9 hours and then stored for approximately 48–72 hrs in a 200:1 solution of PBS:Prohance until they were imaged (Petiet et al., 2007).

MRM was performed at the Duke University Center for In Vivo Microscopy (CIVM) employing a 9.4T vertical bore magnet. The specially-configured system includes Resonance Research coils capable of achieving gradients of 2000 mT/m. Scanning was controlled by a GE MR imaging console (GE Medical Systems, Waukesha, WI) running Epic 12.4 software. This clinical console was adapted for high field (400 MHz) through the use of an intermediate RF up/down converter. Specimens were mounted in a specially fabricated plastic tube and surrounded by fomblin, a perfluorocarbon used to minimize magnetic susceptibility differences at the surface of the specimen. The tube was placed in a 20 mm diameter single sheet solenoid coil. Images were acquired using a conventional refocused spin echo sequence (TR/TE=75/5.2 ms) with an asymmetric partial Fourier sampling strategy to reduce scan time (Johnson et al., 2007). Scan time was approximately 4 hrs for each of the 32 fetal mouse brains examined. Data were reconstructed onto a 512 × 512 × 1024 array. With isotropic spatial resolution at 29 μm, there were approximately 175 sections per brain.

## Fetal Size Analyses

Fetal crown-rump length was assessed in the imaging program ImageJ (Version 1.47, http://rsbweb.nih.gov/ij/) by measuring the length from the crown of the head to the rump in a mid-sagittal MRM image. Whole body volume was also measured in the MRM images using the automatic segmentation feature of ITK Snap (Yushkevich et al., 2006) by placing a seed in the center of the fetal image and allowing it to propagate until the entire fetus was segmented. The 3D segmentation image was then carefully inspected and any mistakes were manually corrected.

### Linear Brain Measurements

The MRM image of each fetus was registered using ImageJ so that each brain was aligned similarly in the horizontal, sagittal and coronal planes. Using the horizontal views, the mid-sagittal brain length, cortical width, frontothalamic length, transverse cerebellar distance, width and length of each olfactory bulb, septal region width and length, pituitary gland width, third ventricle width, and diameter of each eye were measured. These 14 linear measurements were chosen to correlate with previous animal studies and clinical attempts using ultrasound to improve the prenatal diagnostic accuracy of fetuses with developmental ethanol exposure (Godin et al., 2010, Kfir et al., 2009, Parnell et al., 2009). The mid-sagittal brain length was defined as the brain distance from anterior to posterior, minus the olfactory bulbs; the cortical width is the width of the brain from left to right; frontothalamic length is the distance from the anterior aspect of the cortex to the most posterior point of the diencephalon; transverse cerebellar distance is the width of the cerebellum from right to left. All measurements were made at the level of the anterior commissure with the exception of the cerebellum, pituitary, optic globes and olfactory bulbs, which were measured at their widest levels. As previously described, in order to control for potential brain growth retardation, anterior-posterior measurements were normalized to the midsagittal brain length and right-left lengths were normalized to cortical width (Parnell et al., 2009).

### Brain Volumetric Analyses

The volume of 17 brain regions was measured by manually segmenting each of the approximately 175 MRM slices using ITK Snap. The segmented regions (Fig. 1) were defined based on several mouse atlases and include the cerebral cortex, septal region, hippocampus, striatum, diencephalon, olfactory bulbs, midbrain, pons/hindbrain, cerebellum, pituitary, and lateral, third, and combined mesencephalic and fourth ventricular spaces (Schambra, 2008, Schambra et al., 1992, Kaufman, 1992). The right and left olfactory bulbs, cerebral cortices, hippocampi and striata were each considered separately. The individual segmented slices for each region were reconstructed into a 3D structure using ITK Snap. The volume of each region was then recorded and normalized to the overall brain volume to control for individual variability and potential treatment-induced brain growth changes as per Parnell et al., (2009).

### Statistical Analyses

After normalization, the data from the linear and volumetric measurements were analyzed for differences between the ethanol exposure and control groups using a repeated measures ANOVA with each brain region as the repeated measure, as described previously (Parnell et al., 2009, Piven et al., 1996, Yasuno et al., 2002). Upon a finding of significance in the repeated measure ANOVA, post-hoc analyses were performed with a Fisher's protected least significant difference (PLSD). Total body and brain sizes were compared using individual T-tests. Intra-class correlation coefficients (ICC) were used to assess the accuracy and repeatability of the manual segmentations. This test of intra-rater reliability demonstrated that the fetal brains were consistently segmented with all regions above 0.990. All $\alpha$ levels were set at 0.05.

# RESULTS

## General Fetal Characteristics

GD 17 litter sizes, including numbers of live, dead and resorbed fetuses in the control, GD 7–11 and GD 12–16 ethanol-exposure period groups did not differ. The average litter sizes were 9.8, 7.5, 7.2 and 8.0 fetuses for each of the GD 7–11 Ethanol and Control and GD 12–16 Ethanol and Control groups, respectively, with very few resorptions or non-viable fetuses (averaging approximately 1 per litter) in any of the groups.

Data collected for the GD 7–11 period from 12 ethanol-exposed and 5 control GD 17 fetuses (from 7 and 3 litters, respectively) showed no significant differences in whole body size (Control = 545.3 ± 28.5 $mm^3$, Ethanol = 508.8 ± 22.8 $mm^3$ [mean ± standard error]), crown-rump length (Control = 16.85 ± 0.55 mm, Ethanol = 17.01 ± 0.30 mm) or brain volume (Control = 43.9 ± 1.3 $mm^3$, Ethanol = 44.4 ± 0.7 $mm^3$). For the 10 ethanol-exposed and 5 control GD 17 fetuses (from 8 and 2 litters, respectively) examined for the GD 12–16 period, the data showed a body size reduction in the ethanol group. While differences in total fetal volume did not quite reach statistical significance (Control = 543.6 ± 16.5 $mm^3$, Ethanol = 482.7 ± 22.3 $mm^3$; $p = 0.097$), average crown-rump length was significantly less in the ethanol-exposed group than in the controls (Control = 17.62 ± 0.29 mm, Ethanol = 15.84 ± 0.21 mm; $p < 0.001$). However, there were no significant differences in total brain volume (Control = 45.5 ± 1.0 $mm^3$, Ethanol = 41.3 ± 1.6 $mm^3$).

## Linear Brain Measurements

Comparison of linear measurement data from the GD 7–11 treatment and control groups showed that for the 14 measurements made on each GD 17 fetal brain, only that of the right olfactory bulb differed between the groups (Table 1). The average length of the right olfactory bulb in the ethanol-exposed group was about 9% less than that of the controls ($p < 0.01$) Likewise, there were no significant differences in the GD 12–16 treatment and control groups in any linear measurement with the exception of the pituitary gland, which was significantly wider (~9%) in the ethanol-exposed animals ($p < 0.05$) (Table 2).

## Brain Volumetric Analyses

As presented in Figure 2, total and regional brain volume determinations revealed that in the GD 7–11 ethanol-exposure group, the cerebellum was significantly reduced as compared to the controls' ($p < 0.05$). In contrast, the septal region of the ethanol-exposed animals was significantly enlarged ($p < 0.05$). Analyses of the right striatum, hippocampus and olfactory bulb revealed moderate, but non-significant, differences in the volume of these regions ($p = 0.26$, 0.14 and 0.28, respectively). No significant volumetric differences were found for any of the other brain or ventricular regions examined.

In the GD 12–16 ethanol-exposure group the volume of the right hippocampus was significantly reduced ($p < 0.05$) (Fig. 3). This was accompanied by an increase in the volume of the pituitary gland ($p < 0.05$), a finding consistent with the linear measurements. While not quite statistically significant, cerebellar volume was slightly reduced in the ethanol-exposed group ($p = 0.09$). No significant differences were found between the

ethanol-exposed and control groups for any of the other brain or ventricular regions examined.

### Edema

Edema was identified in 7 out of the 10 imaged fetuses that had been ethanol-exposed on GD 12–16 (Fig. 4). These 7 edematous fetuses were derived from 5 separate litters. Severe edema was grossly observable in 2 of the fetuses; each of them presenting with jugular lymphatic sacs that were approximately 3 times larger than controls'. In these severely edematous fetuses, the abnormal fluid accumulation was present throughout the body, including within the pleural and pericardial cavities. In the remaining 5 fetuses, edema was detectable only after MRM imaging. MRM revealed excess fluid accumulation in the nuchal region, with distension of the jugular lymphatic sacs to approximately 2 times the size of controls'. There was an apparent gender bias for this ethanol-induced defect, with 5 of the 7 edematous fetuses (~70%) being female. Edema was not observed in any of the control fetuses or in any that were imaged in the GD 7–11 ethanol exposure group.

## DISCUSSION

The results of this study illustrate that in mice, maternal dietary ethanol intake which results in daily peak BECs of approximately 200 mg/dl and that extends for 5 day periods that are approximately equivalent to weeks 3–6 and 7–12 of human gestation causes exposure period-dependent structural brain damage. This work extends previous MRM-based studies that focused on neuroteratogenic insult occurring on individual days during the earlier of the 2 ethanol exposure periods (i.e. GD 7–11) (Parnell et al., 2013, Godin et al., 2010, O'Leary-Moore et al., 2010, Parnell et al., 2009). In contrast to the previous investigations, the current research paradigm included maternal dietary ethanol intake as opposed to intraperitoneal (ip) administration, with maternal peak BECs that were approximately 50% less than for the acute exposure (individual treatment day) studies. While in the current investigation, significant ethanol-induced changes in linear and volumetric measures were found for specific brain regions, as expected, the number of regions significantly affected and the severity of effect were less than following acute, high dose insult. This expectation was the basis for MRM-based analyses of a relatively large number of ethanol-exposed fetuses for this study. The expense inherent to MRM studies precluded examination of an equal number of control animals; brain volumetric data from which are remarkably consistent among specimens.

Among the GD 7–11 ethanol-exposed fetuses that were analyzed neither body nor brain size significantly differed from controls. Consistent with previous GD 8 and 9 acute-exposure data, a significant decrease in cerebellar volume and a significant increase in septal volume were found in this group of animals. Reduction in septal volume and other defects consistent with holoprosencephaly as result from acute GD 7 ethanol exposure were not identified. This is most likely due to the fact that for induction of these defects peak BECs must occur very early on GD 7, when embryos are just beginning to undergo gastrulation. While in this study dietary ethanol access began at this early time point, it is not likely that sufficient

maternal intake would have occurred during the sensitive period (Zhou et al., 2003, Randall and Taylor, 1979).

In contrast to the GD 7–11 ethanol-exposure group, both crown-rump length and body volume were reduced in the GD 12–16 ethanol-exposed GD 17 fetuses. Together with a trend toward reduction of overall brain volume, width and length, these data indicate that a generalized growth restriction or developmental delay result from ethanol exposure during this later time period. Regional ethanol-induced brain changes for this exposure period included pituitary enlargement and reduction in the volume of the right hippocampus. Regarding the former, previous studies have shown that the pituitary volumes remains constant in control animals on GDs 16,16.5 and 17 (O'Leary-Moore et al., 2010). As a percentage of total brain size, the relative volume of the pituitary actually decreases over this developmental time period indicating that the observed overall developmental delay in this current study does not account for the pituitary size abnormality. Regarding the hippocampal findings, sidedness effects are commonly observed in FASD models. This is especially apparent in tissues outside of the CNS, including the eye and the upper limb, with the right side being more commonly and more severely affected (Parnell et al., 2006, Cook et al., 1987, Chen et al., 2004, Kotch et al., 1992). The significant reduction in the volume of the right hippocampus, along with the trend toward a reduction in the size of the right ocular globe and the right olfactory bulb are in keeping with this right-sided predisposition. It will be of interest to follow up on these findings with behavioral and physiological studies examining hippocampal and pituitary function.

Clearly MRM has proven valuable for neuroteratological analyses. With identification of edema that was not grossly apparent, this study also illustrates the value of this methodology for analyses of other body regions. Indeed, it revealed enlargement of what are apparently the jugular lymphatic sacs in a large proportion of the GD 12–16 ethanol exposure group fetuses. Of interest, development of the lymphatic vascular system has been shown to require adrenomedullin (AM) signaling during this developmental window (Caron and Smithies, 2001), with conditional knockout mice having a reduction in lymphatic endothelial cell proliferation and defects consistent with those in the current investigation (Fritz-Six et al., 2008). How or if ethanol might interfere with AM generation and/or signaling or otherwise might act to cause abnormal lymphatic development, or whether ethanol-induced defects in other cardiovascular structures or organ systems may be the primary cause of edema remains to be determined. That fetal hydrops has been shown in this model system to result from maternal ethanol exposure has obvious clinical implications, supporting the importance of attention to this potential endpoint in assessing ethanol-exposed pregnancies and of considering prenatal ethanol exposure as a causative factor in individuals with this condition.

In conclusion, employing a mouse treatment paradigm that models human ethanol consumption with free dietary access and peak maternal BACs that are commonly achieved with heavy drinking, this work extends our knowledge of ethanol’s teratogenic effects during the human first trimester-equivalent. In particular, it highlights the exposure stage-dependent vulnerability of the septal region, cerebellum, pituitary, and hippocampus and shows that both reductions and increases in the volume of selected brain regions can result

from prenatal ethanol exposure. This study has also identified the end of the human first trimester equivalent as a time when ethanol can cause fetal hydrops, and suggests that this defect deserves more basic and clinical FASD research attention.

## Acknowledgments

This study was conducted at the UNC Bowles Center for Alcohol Studies as part of the Collaborative Initiative on Fetal Alcohol Spectrum Disorders and as part of the Carolina Institute for Developmental Disabilities. It was funded by grant nos. U01-AA017124, U01-AA0216521 and P60-AA011605 to KKS and grant K99/R00-AA018697 to SEP from the National Institute on Alcohol Abuse and Alcoholism/NIH; and by NIBIB grant U54-EB005149-01 and NICHD grant P30-HD03110 to MAS. MRM scanning was performed at the Duke Center for In Vivo Microscopy, an NIH/NIBIB National Biomedical Technology Resource Center (P41-EB015897). The content of this publication is solely the responsibility of the authors and does not necessarily represent the official views of the National Institutes of Health.

## References

Caron KM, Smithies O. Extreme hydrops fetalis and cardiovascular abnormalities in mice lacking a functional Adrenomedullin gene. Proceedings of the National Academy of Sciences of the United States of America. 2001; 98:615–619. [PubMed: 11149956]

Chen SY, Dehart DB, Sulik KK. Protection from ethanol-induced limb malformations by the superoxide dismutase/catalase mimetic, EUK-134. FASEB J. 2004; 18:1234–1236. [PubMed: 15208273]

Coles CD, Smith I, Fernhoff PM, Falek A. Neonatal neurobehavioral characteristics as correlates of maternal alcohol use during gestation. Alcohol Clin Exp Res. 1985; 9:454–460. [PubMed: 3904511]

Cook CS, Nowotny AZ, Sulik KK. Fetal alcohol syndrome. Eye malformations in a mouse model. Arch Ophthalmol. 1987; 105:1576–1581. [PubMed: 3675291]

Cornelius MD, Day NL, Cornelius JR, Geva D, Taylor PM, Richardson GA. Drinking patterns and correlates of drinking among pregnant teenagers. Alcohol Clin Exp Res. 1993; 17:290–294. [PubMed: 8488970]

Floyd RL, Decoufle P, Hungerford DW. Alcohol use prior to pregnancy recognition. Am J Prev Med. 1999; 17:101–107. [PubMed: 10490051]

Fritz-Six KL, Dunworth WP, Li M, Caron KM. Adrenomedullin signaling is necessary for murine lymphatic vascular development. The Journal of clinical investigation. 2008; 118:40–50. [PubMed: 18097475]

Godin EA, O'Leary-Moore SK, Khan AA, Parnell SE, Ament JJ, Dehart DB, Johnson BW, Allan Johnson G, Styner MA, Sulik KK. Magnetic resonance microscopy defines ethanol-induced brain abnormalities in prenatal mice: effects of acute insult on gestational day 7. Alcohol Clin Exp Res. 2010; 34:98–111. [PubMed: 19860813]

Johnson GA, Ali-Sharief A, Badea A, Brandenburg J, Cofer G, Fubara B, Gewalt S, Hedlund LW, Upchurch L. High-throughput morphologic phenotyping of the mouse brain with magnetic resonance histology. Neuroimage. 2007; 37:82–89. [PubMed: 17574443]

Kaufman, MH. The atlas of mouse development. Academic; 1992.

Kfir M, Yevtushok L, Onishchenko S, Wertelecki W, Bakhireva L, Chambers CD, Jones KL, Hull AD. Can prenatal ultrasound detect the effects of in-utero alcohol exposure? A pilot study. Ultrasound Obstet Gynecol. 2009; 33:683–689. [PubMed: 19444822]

Kotch LE, Dehart DB, Alles AJ, Chernoff N, Sulik KK. Pathogenesis of ethanol-induced limb reduction defects in mice. Teratology. 1992; 46:323–332. [PubMed: 1412063]

Lipinski RJ, Hammond P, O'Leary-Moore SK, Ament JJ, Pecevich SJ, Jiang Y, Budin F, Parnell SE, Suttie M, Godin EA, Everson JL, Dehart DB, Oguz I, Holloway HT, Styner MA, Johnson GA, Sulik KK. Ethanol-induced face-brain dysmorphology patterns are correlative and exposure-stage dependent. PLoS One. 2012; 7:e43067. [PubMed: 22937012]

Livy D. Fetal alcohol exposure and temporal vulnerability: effects of binge-like alcohol exposure on the developing rat hippocampus. Neurotoxicology and Teratology. 2003; 25:447–458. [PubMed: 12798962]

Maier SE, Miller JA, Blackwell JM, West JR. Fetal alcohol exposure and temporal vulnerability: regional differences in cell loss as a function of the timing of binge-like alcohol exposure during brain development. Alcohol Clin Exp Res. 1999; 23:726–734. [PubMed: 10235310]

Mooney SM, Miller MW. Vulnerability of macaque cranial nerve neurons to ethanol is time- and site-dependent. Alcohol. 2009; 43:323–331. [PubMed: 19375881]

O'Leary-Moore SK, Parnell SE, Godin EA, Dehart DB, Ament JJ, Khan AA, Johnson GA, Styner MA, Sulik KK. Magnetic resonance microscopy-based analyses of the brains of normal and ethanol-exposed fetal mice. Birth defects research. Part A, Clinical and molecular teratology. 2010; 88:953–964.

O'Rahilly, R.; Fabiola, M. Human Embryology and Teratology. New York, NY: Wiley-Liss; 1992.

Otis EM, Brent R. Equivalent ages in mouse and human embryos. The Anatomical record. 1954; 120:33–63. [PubMed: 13207763]

Parnell SE, Dehart DB, Wills TA, Chen SY, Hodge CW, Besheer J, Waage-Baudet HG, Charness ME, Sulik KK. Maternal oral intake mouse model for fetal alcohol spectrum disorders: ocular defects as a measure of effect. Alcohol Clin Exp Res. 2006; 30:1791–1798. [PubMed: 17010146]

Parnell SE, Holloway HT, O'Leary-Moore SK, Dehart DB, Paniaqua B, Oguz I, Budin F, Styner MA, Johnson GA, Sulik KK. Magnetic resonance microscopy-based analyses of the neuroanatomical effects of gestational day 9 ethanol exposure in mice. Neurotoxicology and Teratology. 2013; 39:77–83. [PubMed: 23911654]

Parnell SE, O'Leary-Moore SK, Godin EA, Dehart DB, Johnson BW, Allan Johnson G, Styner MA, Sulik KK. Magnetic resonance microscopy defines ethanol-induced brain abnormalities in prenatal mice: effects of acute insult on gestational day 8. Alcohol Clin Exp Res. 2009; 33:1001–1011. [PubMed: 19302087]

Petiet A, Hedlund L, Johnson GA. Staining methods for magnetic resonance microscopy of the rat fetus. J Magn Reson Imaging. 2007; 25:1192–1198. [PubMed: 17520739]

Piven J, Arndt S, Bailey J, Andreasen N. Regional brain enlargement in autism: a magnetic resonance imaging study. Journal of the American Academy of Child and Adolescent Psychiatry. 1996; 35:530–536. [PubMed: 8919716]

Randall CL, Taylor WJ. Prenatal ethanol exposure in mice: teratogenic effects. Teratology. 1979; 19:305–311. [PubMed: 473082]

Sawant OB, Lunde ER, Washburn SE, Chen WJ, Goodlett CR, Cudd TA. Different patterns of regional Purkinje cell loss in the cerebellar vermis as a function of the timing of prenatal ethanol exposure in an ovine model. Neurotoxicology and Teratology. 2013; 35:7–13. [PubMed: 23195754]

Schambra, UB. Prenatal mouse brain atlas. New York: Springer; 2008.

Schambra, UB.; Lauder, JM.; Silver, J. Atlas of the prenatal mouse brain. San Diego: Academic Press; 1992.

Schneider ML, Moore CF, Adkins MM. The effects of prenatal alcohol exposure on behavior: rodent and primate studies. Neuropsychol Rev. 2011; 21:186–203. [PubMed: 21499982]

Schoenwolf, GC.; Bleyl, SB.; Brauer, PR.; Francis-West, PH. Larsen's Human Embryology. 4 ed.. Philadelphia, PA: Churchhill Livingstone; 2009.

Strachan, T.; Lindsay, S.; Wilson, DI. Molecular Genetics of Early Human Development, in Series Molecular Genetics of Early Human Development. In: Cooper, DN.; Humphries, SE.; Strachan, T., editors. The Human Molecular Genetics Series. Oxford, UK: BIOS Scientific Publishers; 1997.

Sulik KK. Genesis of alcohol-induced craniofacial dysmorphism. Exp Biol Med (Maywood). 2005; 230:366–375. [PubMed: 15956766]

Sulik KK, Johnston MC, Webb MA. Fetal alcohol syndrome: embryogenesis in a mouse model. Science. 1981; 214:936–938. [PubMed: 6795717]

Theiler, K. The house mouse : atlas of embryonic development. New York: Springer-Verlag; 1989.

Workman AD, Charvet CJ, Clancy B, Darlington RB, Finlay BL. Modeling transformations of neurodevelopmental sequences across mammalian species. The Journal of neuroscience : the official journal of the Society for Neuroscience. 2013; 33:7368–7383. [PubMed: 23616543]

Yasuno F, Hasnine AH, Suhara T, Ichimiya T, Sudo Y, Inoue M, Takano A, Ou T, Ando T, Toyama H. Template-Based Method for Multiple Volumes of Interest of Human Brain PET Images. Neuroimage. 2002; 16:577–586. [PubMed: 12169244]

Yushkevich PA, Piven J, Hazlett HC, Smith RG, Ho S, Gee JC, Gerig G. User-guided 3D active contour segmentation of anatomical structures: significantly improved efficiency and reliability. Neuroimage. 2006; 31:1116–1128. [PubMed: 16545965]

Zhou FC, Sari Y, Powrozek T, Goodlett CR, Li TK. Moderate alcohol exposure compromises neural tube midline development in prenatal brain. Brain Res Dev Brain Res. 2003; 144:43–55.

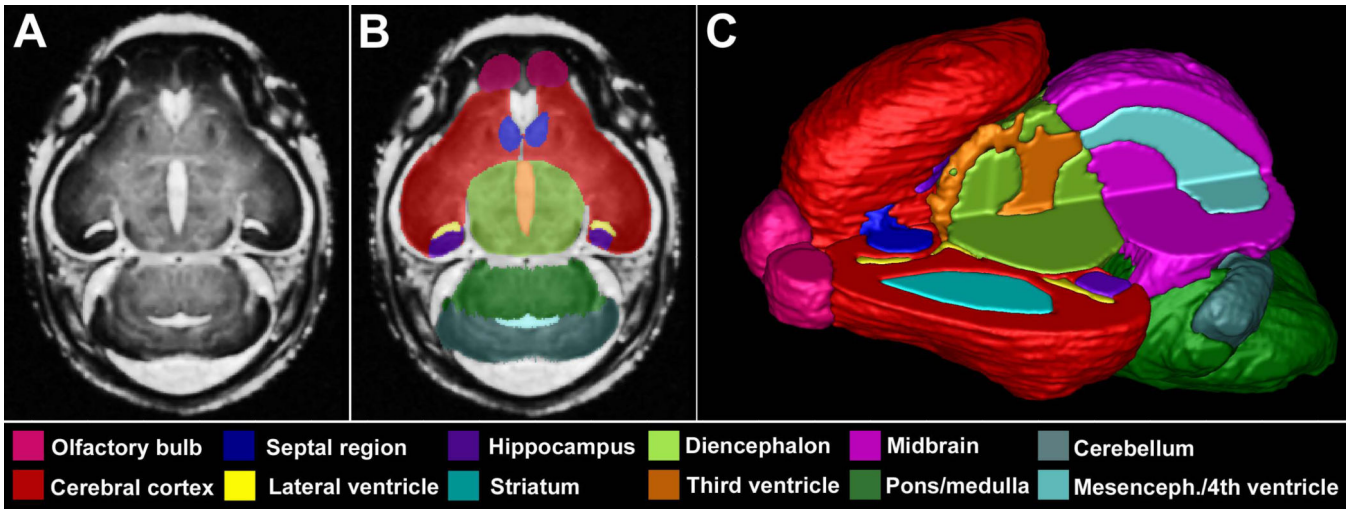


**Figure 1.**

Manually segmented magnetic resonance microscopy (MRM)-derived images of the GD 17 mouse brain. A representative coronal MRM view (A) demonstrates the high resolution made possible with this imaging technology. Manually segmented MRM scans are regionally color-coded (B). 3-D reconstructions are generated (C) for use in evaluating gross morphology, calculating regional volumes and analyzing potential shape changes. Notice that the upper left quadrant of the reconstructed brain was removed to allow visualization of the internal structures.

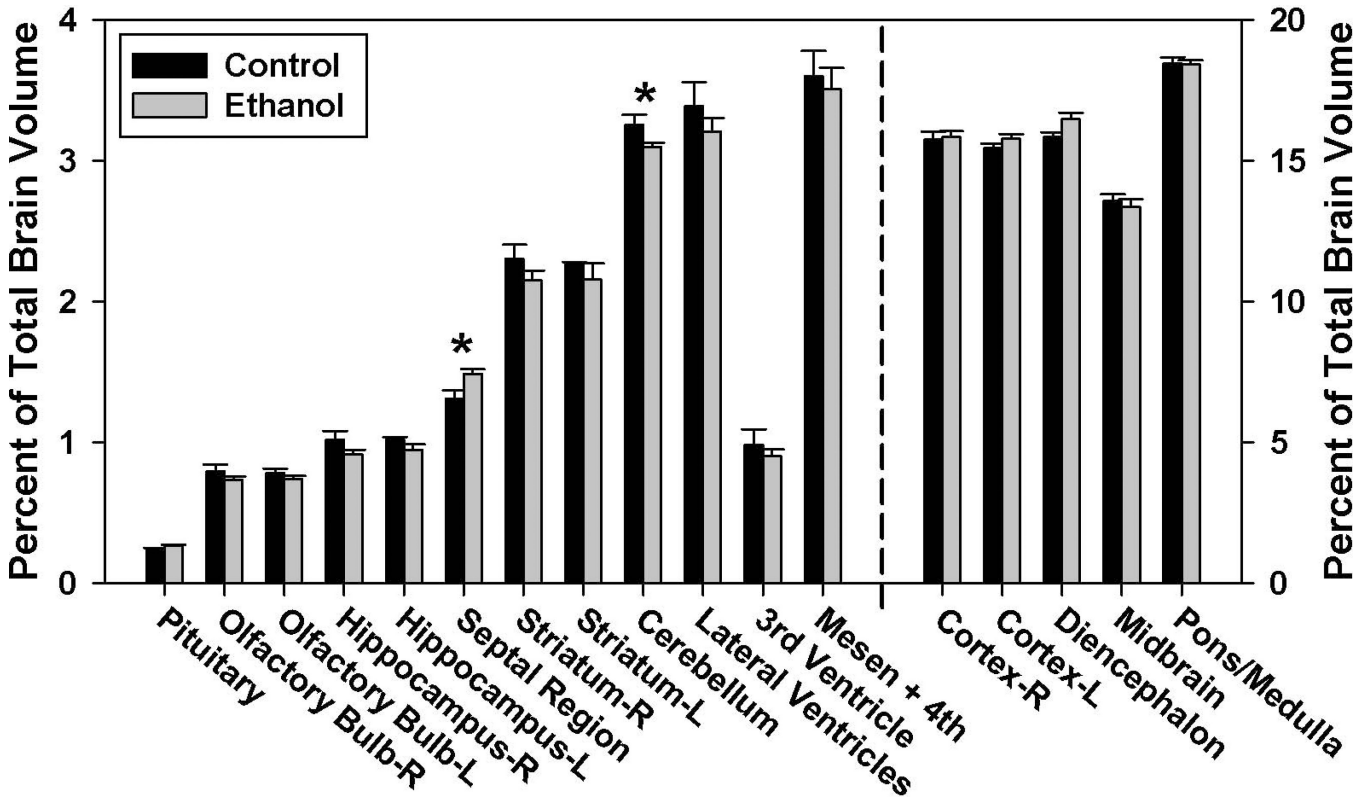


**Figure 2.**

Ethanol-induced regional volumetric changes resulting from GD 7–11 maternal dietary ethanol exposure. Regional GD 17 brain volumes are shown as a percentage of total brain volume and are graphed using two different scales in order to adequately convey the findings, with the structures to the left of the dashed line requiring a smaller scale than those on the right. The early first trimester equivalent ethanol exposure significantly reduced the volume of the cerebellum, while increasing the volume of the septal region. There were no significant volumetric differences between the ethanol (n=12) and control (n=5) groups in the other regions examined ($p < 0.05$).

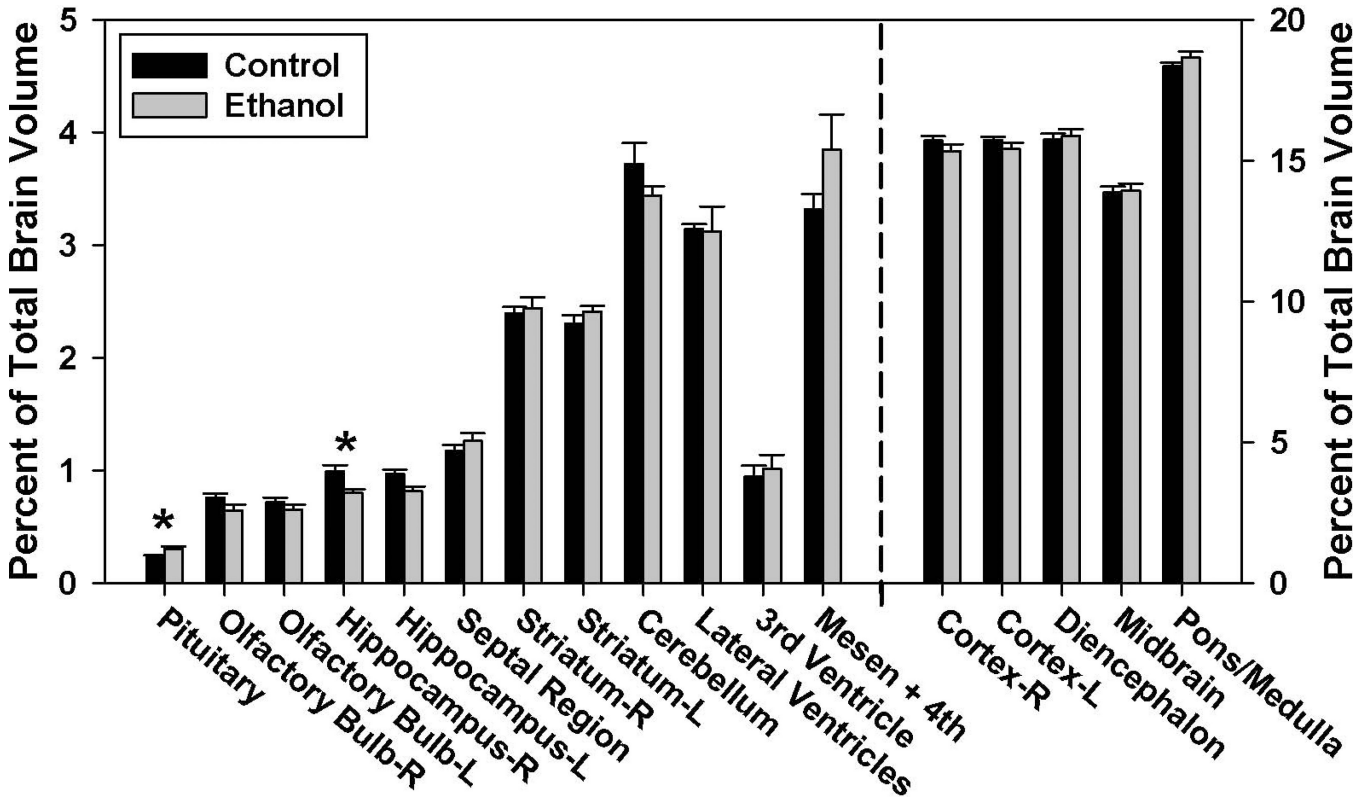


**Figure 3.**

Ethanol-induced regional volumetric changes resulting from GD 12–16 maternal dietary alcohol exposure. Regional GD17 brain volumes are shown as a percentage of total brain volume and are graphed using two different scales in order to adequately convey the findings, with the structures to the left of the dashed line requiring a smaller scale than those on the right. The late first trimester equivalent ethanol exposure significantly reduced the volume of the right hippocampus, while increasing the volume of the pituitary. An increase in the volume of the mesencephalic and 4th ventricles approached, but did not reach significance. No significant volumetric differences were found between the ethanol (n=10) and control (n=5) groups in the other regions examined. ($p < 0.05$).

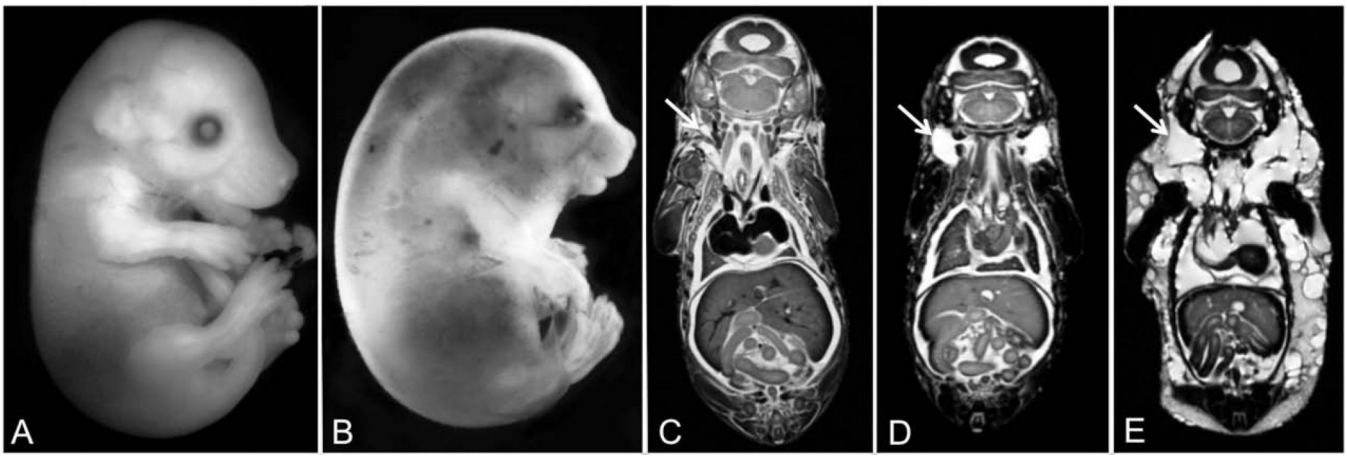


**Figure 4.**

As apparent grossly and/or with MRM, GD 12–16 maternal dietary ethanol exposure induced varying degrees of fetal edema. In contrast to the control GD 17 fetus shown in (A), the ethanol-exposed fetus shown in (B) is severely edematous, with excess fluid accumulation being particularly evident in the nuchal region. Comparison of MRM images of a control (C), moderately (D), and severely affected (E) fetus illustrates normally appearing, moderately distended and grossly distended jugular lymphatic sacs (arrows), respectively). The fetus shown in (E) also presents with obvious edema throughout the body including the pleural and pericardial cavities.

## Table 1

### GD 7–11 Linear Measurements

Linear measurements in GD 7–11 control and ethanol-exposed fetal mice. Crown-rump length, mid-sagittal brain length and cortical width data are presented in real mm measurements. All other data is expressed as a percentage of either mid-sagittal brain length (for anterior/posterior measurements) or cortical width (for left-right measurements). Only the length of the right olfactory bulb was significantly different between ethanol-exposed subjects and controls.

| Measurement (mean ± sem) | Control | Ethanol |
|---|---|---|
| Crown-rump length (mm) | 16.85 ± 0.55 | 17.01 ± 0.30 |
| Mid-sagittal brain length (mm) | 6.37 ± 0.05 | 6.39 ± 0.09 |
| Cortical width (mm) | 4.28 ± 0.05 | 4.31 ± 0.02 |
| Frontothalamic length | 50.23 ± 0.32 | 48.89 ± 0.42 |
| Olfactory bulb length | | |
| Right | 13.34 ± 0.23 | 12.17 ± 0.17 * |
| Left | 13.37 ± 0.24 | 12.55 ± 0.25 |
| Olfactory bulb width | | |
| Right | 19.37 ± 0.31 | 19.20 ± 0.24 |
| Left | 18.69 ± 0.49 | 18.79 ± 0.29 |
| Septal region length | 14.33 ± 0.18 | 14.55 ± 0.27 |
| Septal region width | 24.30 ± 0.17 | 24.72 ± 0.24 |
| Pituitary width | 25.20 ± 0.83 | 23.70 ± 0.52 |
| Third ventricle width | 5.60 ± 0.60 | 5.71 ± 0.29 |
| Cerebellar width | 75.21 ± 0.15 | 74.80 ± 0.32 |
| Ocular width | | |
| Right | 26.21 ± 0.36 | 26.12 ± 0.34 |
| Left | 26.12 ± 0.31 | 26.16 ± 0.34 |

* Indicates $p < 0.005$

## Table 2

### GD 12–16 Linear Measurements

Linear measurements in GD 12–16 control and ethanol-exposed fetal mice. Crownrump length, mid-sagittal brain length and cortical width data are presented in real mm measurements. All other data is expressed as a percentage of either mid-sagittal brain length (for anterior/posterior measurements) or cortical width (for left-right measurements). Only the width of the pituitary gland and crown-rump length were significantly different between ethanol-exposed subjects and controls.

| Measurement (mean ± sem) | Control | Ethanol |
|---|---|---|
| Crown-rump length (mm) | 17.62 ± 0.29 | 15.86 ± 0.21 * |
| Mid-sagittal brain length (mm) | 6.46 ± 0.06 | 6.16 ± 0.11 |
| Cortical width (mm) | 4.29 ± 0.04 | 4.16 ± 0.08 |
| Frontothalamic length | 48.14 ± 0.36 | 47.67 ± 0.35 |
| Olfactory bulb length | | |
| Right | 12.30 ± 0.61 | 11.79 ± 0.15 |
| Left | 12.93 ± 0.57 | 12.09 ± 0.30 |
| Olfactory bulb width | | |
| Right | 18.38 ± 0.16 | 18.36 ± 0.43 |
| Left | 18.40 ± 0.33 | 18.58 ± 0.35 |
| Septal region length | 13.95 ± 0.17 | 14.81 ± 0.44 |
| Septal region width | 25.29 ± 0.33 | 25.77 ± 0.37 |
| Pituitary width | 25.08 ± 0.67 | 27.43 ± 0.51 * |
| Third ventricle width | 6.13 ± 0.41 | 7.02 ± 0.58 |
| Cerebellar width | 76.19 ± 0.38 | 75.76 ± 0.72 |
| Ocular width | | |
| Right | 26.60 ± 0.36 | 25.71 ± 1.18 |
| Left | 26.30 ± 0.54 | 26.79 ± 1.07 |

* Indicates $p < 0.05$